




# Shock wave-induced defect engineering on structural and optical properties of crown ether magnesium chloride potassium thiocyanate single crystal

K. Showrilu<sup>1,\*</sup> , Ch. Jyothirmal<sup>1</sup>, A. R. N. L. Sirisha<sup>1</sup>, A. Sivakumar<sup>2</sup>, S. Sahaya Jude Dhas<sup>3</sup>, and S. A. Martin Britto Dhas<sup>2</sup>

<sup>1</sup>Department of Physics, Ch. S. D. St. Theresa College (A) for Women, West Godavari, Eluru, Andhra Pradesh 534 003, India

<sup>2</sup>Shock Wave Research Laboratory, Department of Physics, Abdul Kalam Research Centre, Sacred Heart College, Tirupattur, Tamilnadu 635 601, India

<sup>3</sup>Department of Physics, Kings Engineering College, Sriperumbudur, Chennai, Tamilnadu 602 117, India

**Received:** 13 October 2020

**Accepted:** 16 December 2020

**Published online:**

11 January 2021

© The Author(s), under exclusive licence to Springer Science+Business Media, LLC part of Springer Nature 2021

## ABSTRACT

In the present work, a successful attempt was made to synthesize 18-crown-6-ether magnesium chloride potassium tris-thiocyanate (CMPTC) which was grown as the single crystal with the dimensions of  $12 \times 2 \times 1 \text{ mm}^3$  by slow evaporation method. The prominent properties of CMPTC single crystal, namely crystallographic structure, surface morphology, and optical transmittance, were estimated using powder X-ray diffraction, optical microscope, and UV–Visible spectrometer, respectively. The effect of shock waves on CMPTC single crystal was explored by loading with specific shock pulses of 1, 2, and 3 having Mach number 1.7. The XRD studies reveal that diffraction peaks of the test crystal have undergone a lower angle shift with respect to number of shocks due to the reduction of crystalline nature. The optical transmittance study reveals that the sample loses the optical transmission significantly by the dynamic impact of shock waves due to the formation of surface defects and cracks which is also reflected in the optical microscopic images providing the supporting evidence for the changes occurring at shocked conditions. From the shock wave impact study, we conclude that the title compound of CMPTC is not suitable for the applications of electronic device fabrications intended to be working under high pressure and high temperature.

Address correspondence to E-mail: kondaveetishowri@gmail.com

## 1 Introduction

The impact of high-energetic waves and rays (X-rays, gamma rays, electron irradiation, electromagnetic waves, shock waves, etc.) on the physical and chemical properties of crystalline and non-crystalline materials is witnessed to have attained remarkable attention from material science researches in the last few decades [1–3]. Predominantly, shock wave-induced analysis of the properties of crystalline materials has been paid greater attention by the researchers due to the simplicity of the experimental method which is capable of inducing astounding changes in material properties during the shock wave propagation through the materials. In general, shock wave-induced technique is being used to investigate the stability of materials against high-temperature and high-pressure conditions. Shock waves can constitute an environment which is equivalent to the extreme environmental conditions such as very high pressure, temperature, stress, tension, and force simultaneously in a single shock pulse [4–8]. Due to this advantage, reasonably extensive research is observed to be in progress centred on investigations of material properties under shock wave-loaded conditions so as to be utilized for aerospace applications. Generally, low weight and high structural and mechanical stabilities are the essential requirements for the materials to be used in space, military, defence, and nuclear power plant applications. When space missiles enter into space, it is possible that they are affected by the presence of radiation and shock waves. Similarly, in military and defence, the electronic devices used are likely to be exposed to shock waves emanated from bomb explosions, collisions, etc. If materials are susceptible to shock waves and undergo mechanical and structural instabilities, the efficiency of the device would be affected significantly. Hence, the electronic device engineers are looking forward to the materials which have high structural stability so as to safeguard against shock-waves [9–11]. Non-linear optical (NLO) crystals are primarily used in aerospace, military, defence, and technological applications such as data transmission, frequency conversions, signal processing, optical modulation, and high-power laser applications [12–14]. So far, much of the work has been going on in crystal growth and characterization of materials that have been used for the above-said applications in ambient conditions. However, identifying single

crystals that could be used in space environment-based electronic devices with high performance might be a multi-million dollar question. For this reason, searching for the materials of high stability which could withstand the above-said extreme environmental conditions and also to satisfy the requirements of specific applications is a burning research topic. The properties of ammonium dihydrogen phosphate (ADP), potassium dihydrogen phosphate (KDP), tri-glycine sulphate (TGS), glycine phosphate (GPI), and benzyl crystals have been investigated under the action of shock waves [15–21]. Among the listed single crystals, KDP crystal exhibits relatively stable material properties after confronting the impact of shock waves. On the other hand, ADP, benzyl, and copper sulphate crystals show the enhancement of optical properties during the shock wave propagation due to the re-crystallization mechanism [22]. Furthermore, dye-doped KDP crystals (rhodamine B and methylene blue dyes) have been investigated under the impact of shock waves which have reflected that both the crystals have undergone significant reduction of optical transmittance and optical bandgap energy with respect to number of shock pulses [23, 24].

From these observations, it can be generalized that, during the impact of shock waves, many physico-chemical properties become altered and the changes depend on the molecular and structural properties of the materials. Followed by the investigations of these NLO crystals, crown ether magnesium chloride potassium thiocyanate crystal has been selected for the shock wave recovery experiment. It is one of the potential semi-organic NLO materials that belongs to the hexagonal crystal system [25–27]. Quite a few articles have been published so far on the crystal growth and characterization of the sample at ambient conditions. But there is no article found in the literature featuring shock effects, gamma irradiation, and other high-energy ray irradiation conditions exposed on CMPTC crystal. This study aims at analysing the impact of the shock wave on the structural and optical properties of the title crystal.

## 2 Experimental section

### 2.1 Crystal growth

The single crystal of CMPTC was synthesized by slow evaporation technique. The AR grade chemicals of crown ether, magnesium chloride, and potassium thiocyanate were taken with 1:1:1 ratio in 50 ml solution of water. The solution was stirred utilizing a magnetic stirrer for 3 h to get the homogenous saturated solution. After preparing the saturated solution, it was filtered into a glass beaker by a filter paper. Then, it was covered with a perforated polythene sheet and kept aside for enabling slow evaporation at ambient temperature. Within a week, a colourless, transparent, and thin hexagonal single crystal with the dimensions of  $12 \times 2 \times 1 \text{ mm}^3$  was obtained and the photograph of the as grown single crystal is shown in Fig. 1.

### 2.2 Shock wave loading

For the present experiment, we have used the shock waves of Mach number 1.7 so as to investigate the structural and optical stabilities of the title compound (CMPTC). The cut and well-polished ( $\sim 1 \text{ mm}$  thickness) test sample has been chosen for the experiment and the shock waves of transient pressure 1.0 MPa have been loaded on it. The working methodology of shock tube and the procedure of shock wave loading have been explained in our previous publications [8, 9]. Briefly, the shock tube has three sections such as driver, driven, and diaphragm sections. Atmospheric air has been used as



**Fig. 1** The photograph of the grown CPMTC crystal

the input source for the required shock wave generation. While the atmospheric air is compressed into the driver section, at the critical pressure, the diaphragm is ruptured and the shock wave is generated and it moves along the driven section [28]. The test samples have been placed one by one with a regular interval between them in the sample holder which is placed 1 cm away from the open end of the shock tube. Subsequently, 1, 2, and 3 shock pulses have been loaded on the sample such that the structural, optical, and morphological properties have been analysed and the obtained results are to be discussed in the following sections.

## 3 Result and discussion

### 3.1 Structural properties

The structural properties of the control and shock wave-loaded test crystals have been evaluated by D2-phasor Bruker X-ray diffractometer (2019) ( $\text{Cu K}\alpha$ ) over the diffraction angle between 10 and 80 degrees with the step increment of 0.01 degree. During the XRD measurement, the cut and polished test crystal (1 mm thickness) has been placed in the sample holder and the diffraction profile has been recorded. The obtained powder XRD profiles of the control and shock wave-loaded CPMTc crystals are shown in Fig. 2.

As seen in Fig. 2, the control sample has five diffraction peaks such as (001), (002), (003), (004), and

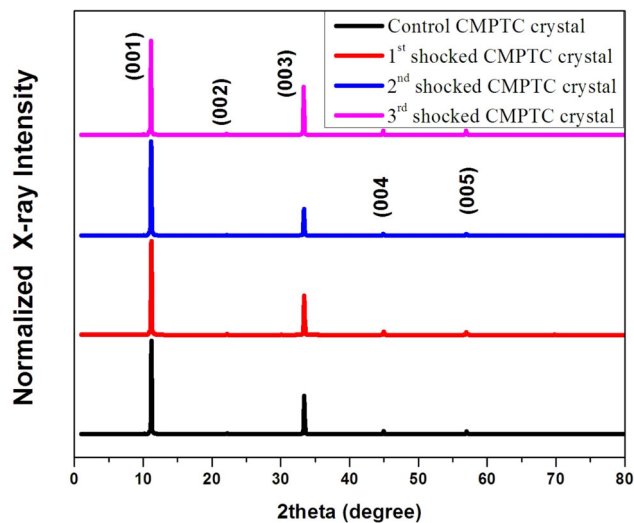


**Fig. 2** PXRD profiles of the control and shocked CPMTc crystals

(005) over the diffraction angle from 10 to 80°. Among the two prominent planes, the diffraction peak (001) has high X-ray intensity and (003) has low X-ray intensity. In principle, the diffraction profile should exhibit the maximum intensity only at 11.224 degree that has to be the characteristics of the particular plane (001) of the single crystal. So, the other diffraction peaks are considered to be second- and third-order diffraction planes. As seen in the diffraction peaks of Fig. 2, no new peak appears or the existing peak disappears by the impact of shock waves in accordance with the number of shock pulses. However, a small peak shifting as well as peak broadening have occurred because of the impact of shock waves as reflected in Fig. 3. Based on the visibility of the diffraction peaks, the first and the third peaks are taken into account so as to evaluate the shock wave-induced effects and the selected diffraction peaks are denoted in Fig. 3. In the first step, we have considered the sharp diffraction peak for the investigation of shock wave-induced changes and the corresponding diffraction peak is shown in Fig. 3a. As seen in Fig. 3a, there are slight changes that are

observed in peak broadening as well as shifting in accordance with number of shock waves. While the number of shock pulses is increased, the test crystal undergoes a shift towards lower angle which is due to the considerable amount of distortions occurring in the particular crystalline system [10–16]. The (001) peak positions are identified to be at 11.224°, 11.192°, 11.161°, and 11.127° for the control, first, second, and third shocked conditions, respectively. The crystallite size has been calculated for the control and shocked crystals and the observed values are 74 nm, 57 nm, 57 nm, and 95 nm. The observed changes have been enforced in the crystallite size due to the dynamic impact of shock waves.

Secondly, we have considered a higher-order diffraction peak (003) for the assessment of impact of shock resistance and the corresponding diffraction peaks are presented in Fig. 3b. Additionally, we have observed similar changes occurring in few more diffraction peaks such as peak broadening and lower angle shift and the corresponding values of higher-order diffraction peak positions are found to be 33.415°, 33.415°, 33.381°, and 33.347° with respect to

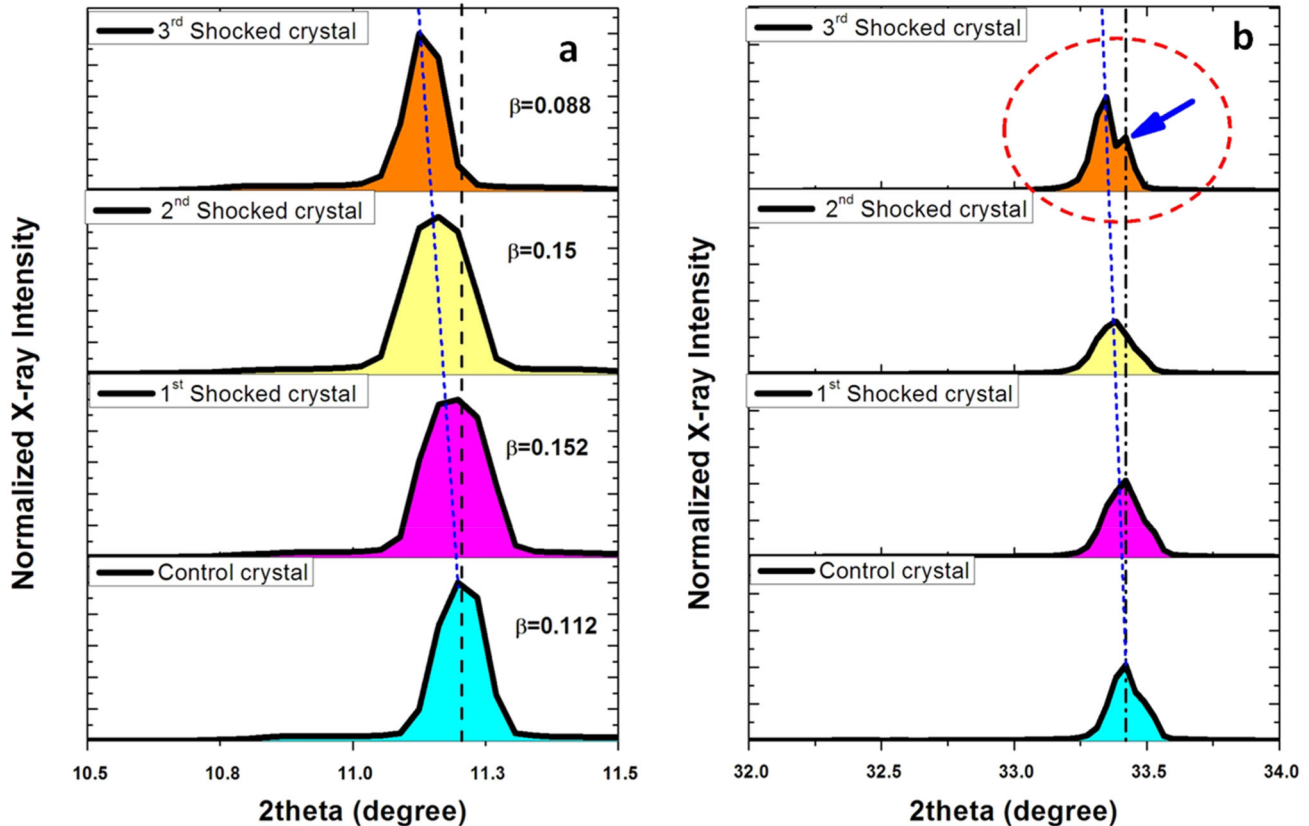


Fig. 3 Selected region of diffraction angle in the PXRD profile for the control and shocked CPMTc crystals

the control, first, second, and third shocked conditions. Moreover, in the case of (003) plane, at 3<sup>rd</sup> shock, there is a shoulder peak appearance that is created by the impact of shock waves and it also represents the occurrence of deformations and distortions in the test crystal. As per the crystallographic structure of the test crystal, Mg(SCN)<sub>3</sub>·4H<sub>2</sub>O units are hydrogen bonded through the four water molecules to the 18-crown-6 rings. Generally, at high pressure and shocking conditions, the hydrogen-bonded materials undergo remarkable changes in the crystal system [17–24, 29].

### 3.2 Optical properties

The stability of optical properties such as optical transmittance of NLO materials are highly required before considering them for real-time applications, especially for high-power laser applications and space-based electronic devices. So, we have focussed our special attention to investigate the stability of optical properties of the test crystal at shocked conditions. The test crystals' optical transmission has been recorded over the wavelength range between 200 and 800 nm using a Varian Cary 5E spectrometer (Varian, 2010) keeping air medium as the reference. The optical transmittance spectra of the control and shocked crystals are shown in Fig. 4. The control test crystal has 72% of optical transmittance at 800 nm that is a highly favourable property required for the electro-optical applications. Consequently, shock wave-loaded test crystals have undergone

considerable changes in the values of optical transmittance in the same wavelength region and the observed changes of optical transmittance are very well reflected in the profiles as shown in Fig. 4.

As seen in Fig. 4, unexpectedly the optical transmittance is significantly reduced with respect to number of shock pulses. Figure 5 shows the relation between number of shock pulses and optical transmittance at 800 nm wavelength. In our previous work, we have observed a lot of changes in optical transmittance in various crystals such as ammonium dihydrogen phosphate [17], tri-glycine sulphate [19], benzil [21], and copper sulphate [22]. When benzyl

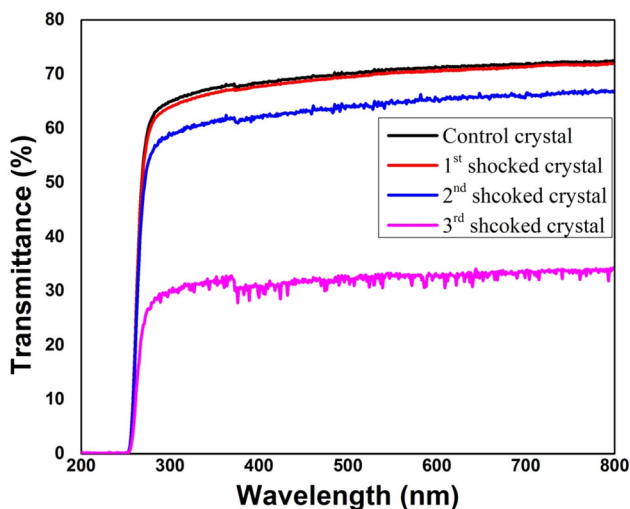


**Fig. 4** Optical transmittance spectra of the control and shock wave-loaded crystals

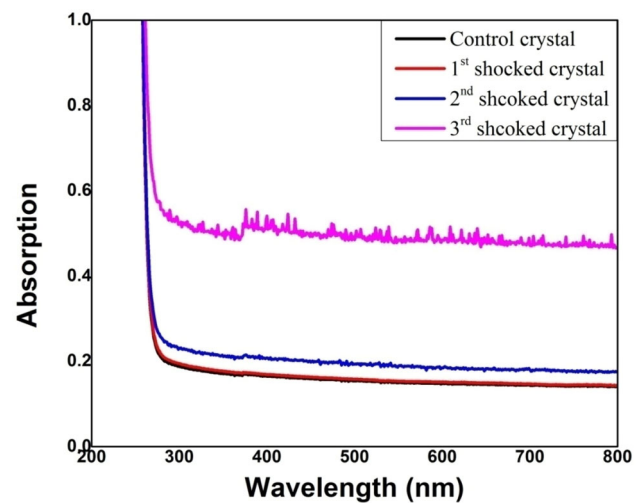


**Fig. 6** Optical absorption spectra of the control and shocked crystals

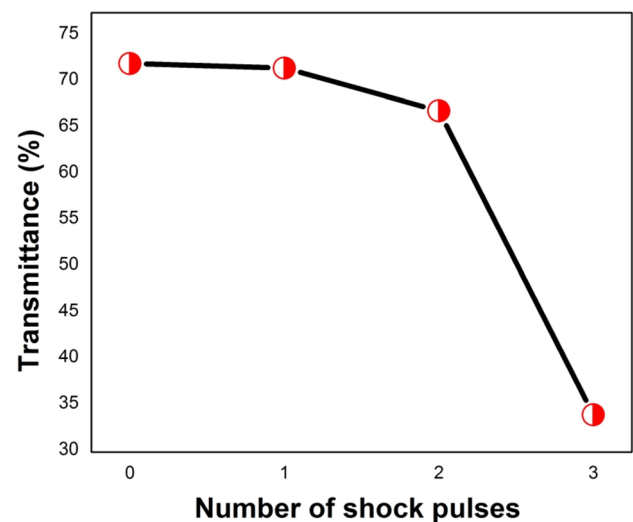


**Fig. 5** Transmittance vs number of shock pulses at 800 nm wavelength

and copper sulphate crystals are allowed for dynamic re-crystallization between the internal grain boundaries enforced with shock wave loading, the optical transmittance is found to have increased [21, 22]. On the other hand, ammonium dihydrogen phosphate and tri-glycine sulphate crystals' optical transmittance has reduced [17, 19]. In the present experiment, we have observed the loss of optical transmittance with respect to the number of shock pulses, i.e. from 72 to 34%. The loss of optical transmittance may be due to the formation of microcracks, voids, distortion, and deformations, as well as surface damages. In powder XRD results, we have found the creation of lattice distortions and deformations at shocking conditions and these effects might have led to the significant reduction of optical transmittance.

Moreover, we have also observed an unusual behaviour in optical transmittance spectra at shocked conditions. While looking at the optical transmittance data of the control test crystal, there is no data fluctuation observed and the corresponding line is highly smooth. But in shock wave-loaded conditions, the data fluctuations have significantly increased with respect to the number of shocks. At 3rd shock, the degree of variation has increased substantially which is reflected in the surface of the test crystal that has been considerably damaged due to the exposure of shock waves. The surface morphology analysis has been used to ensure surface details of the test crystal having encountered with shock waves. Moreover, surface morphology analysis provides the alternative track to understand the changes occurring in optical transmittance of the test crystal for the applied shock pulses. Furthermore, the optical absorption and optical bandgap energy of the control and shocked

crystals have been calculated and the corresponding profiles are presented in Figs. 6 and 7. As seen in Fig. 7, the absorption values are found to be linearly increasing with respect to the number of shocks pulse which clearly indicates the formation of surface defects and cracks influenced by the impact of shock waves and similar results have been observed in TGS crystal [19].

Optical bandgap energy of the control and shocked crystals has been calculated by Tauc plot relation [30, 31] and the calculated values are 4.83 eV, 4.83 eV, 4.83 eV, and 4.80 eV for the control, first, second, and third shock wave-loaded crystals, respectively. No significant optical bandgap energy change has been observed.

### 3.3 Surface morphology

Optical microscopic analysis is a simple and efficient method to ensure the surface changes that have occurred in optically transparent materials under deforming forces. Weswox optical microscopy (WESWOX, BX-LTR, 2010) has been used to analyse the shock wave-induced changes on the title crystals' surface and the observed micrographs are shown in Fig. 6. As seen in Fig. 8a, it is clear that the control crystal surface has no visible damages and defects. In shock wave-loaded conditions, the test crystal suffers with surface damages and cracks. Additionally, from the observed micrographs, it could be noted that the defect area increases with respect to number of shock waves. After the administration of the 3rd shock, a higher damage is observed on the test crystal surface that might have resulted in the significant reduction

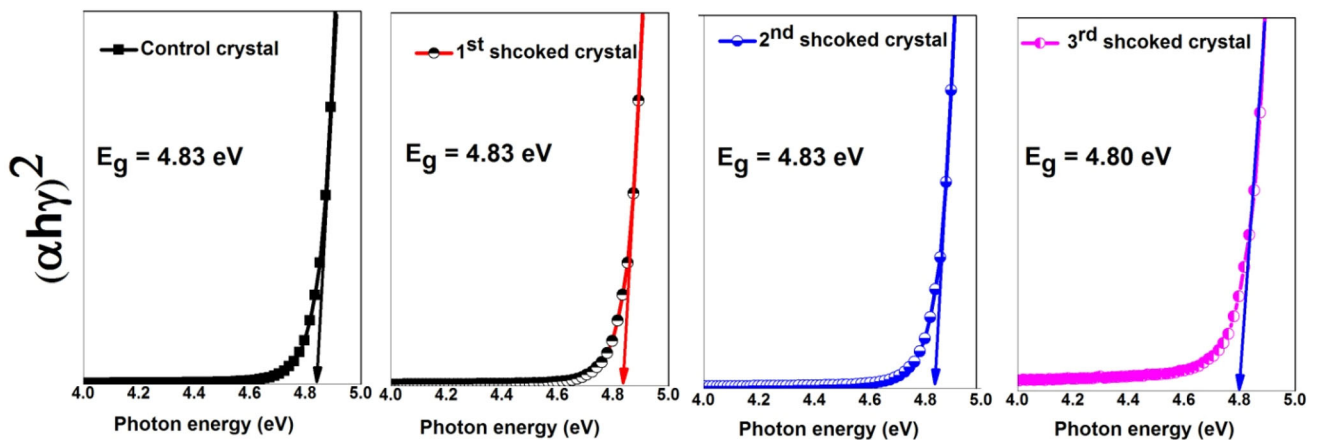
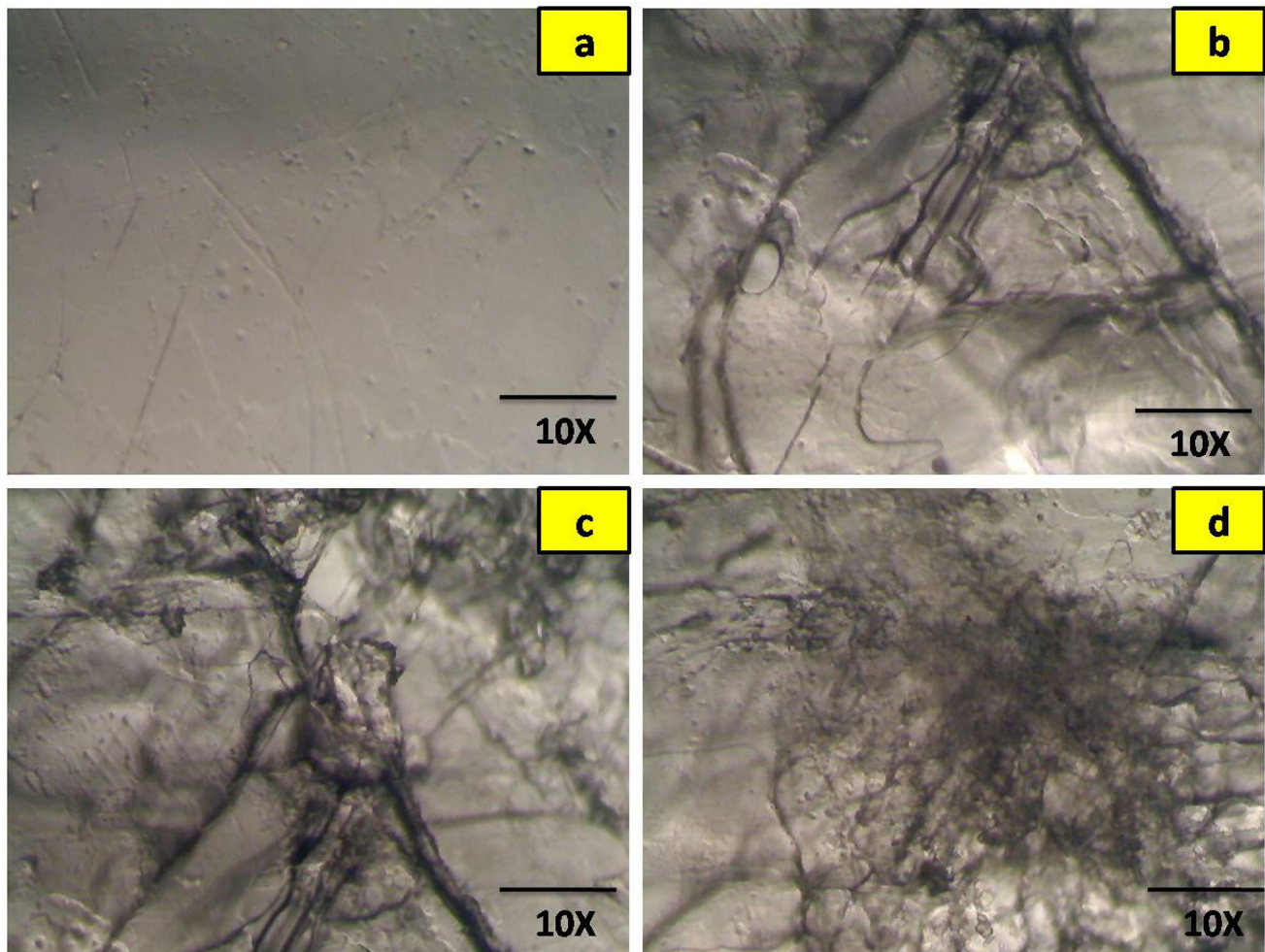


Fig. 7 Optical bandgap energy of the control and shocked crystals



**Fig. 8** Optical micrographs of the control and shocked CPMTC crystals: **a** the control, **b** 1st shocked, **c** 2nd shocked, **d** 3rd shocked

of optical transmittance due to the enhancement of the scattering of incident light [19].

#### 4 Conclusion

The single crystal of CPMTC was grown by slow evaporation technique. The structural, morphological stability and optical properties of CPMTC were studied for both the control and shock wave-loaded crystals systematically. The PXRD results show that the test crystal does not undergo any structural phase transition at shocked conditions. Moreover, it is observed that surface defects and cracks have been developed under the shock wave treatment. Moreover, the UV–Vis–NIR spectral results confirm that the test crystals' optical transmittance decreases while increasing the number of shock waves. The observed reduction of optical transmittance is due to

the formation of cracks and voids in the title crystal influenced by the impact of shock waves. Optical micrographs provide the alternate proof to understand better the changes occurring in the structural and optical properties of the test crystal at shocked conditions. Based on the above-mentioned factors, it could be concluded that the test crystal's structural and optical properties are not stable at shocked conditions. Hence, the grown single crystal of CPMTC may not be the right candidate for the aerospace and high-pressure applications.

#### References

1. K. Ichianagi, S. Takagi, N. Kawai, R. Fukaya, S. Nozawa, K.G. Nakamura, K.-D. Liss, M. Kimura, S.-I. Adachi,

- Microstructural deformation process of shock-compressed polycrystalline aluminium. *Sci. Rep.* **9**, 7604 (2019)
2. A.V. Krasheninnikov, K. Nordlund, Ion and electron irradiation-induced effects in nanostructured materials. *J. Appl. Phys.* **107**, 071301 (2010)
  3. D. Joseph Daniel, U. Madhusoodanan, R. Nithya, P. Ramasamy, Irradiation effect on luminescence properties of fluoroperovskite single crystal (LiBaF<sub>3</sub>:Eu<sup>2+</sup>). *Rad. Phys. Chem.* **96**, 135–139 (2014)
  4. A. Rita, A. Sivakumar, S. Sahaya Jude Dhas, S.A. Martin Britto Dhas, Reversible magnetic phase transitions of MnO<sub>2</sub> nano rods by shock wave recovery experiments. *J. Mater. Sci.: Mater. Electron.* (2020). <https://doi.org/10.1007/s10854-020-04555-5>
  5. Z.-H. He, J. Chen, G.-F. Ji, L.-M. Liu, W.-J. Zhu, Q. Wu, Dynamic responses and initial decomposition under shock loading: a DFTB calculation combined with MSST method for  $\beta$ -HMX with molecular vacancy. *J. Phys. Chem. B* **119**, 10673–10681 (2015)
  6. Y. Yao, Z. Huang, P. Xie, L. Wu, L. Ma, T. Li, Z. Pang, M. Jiao, Z. Liang, J. Gao, Y. He, High temperature shockwave stabilized single atoms. *Nat. Nanotechnol.* **14**, 857 (2019)
  7. F. Bai, K. Bian, X. Huang, Z. Wang, H. Fan, Pressure induced nanoparticle phase behavior, property, and applications. *Chem. Rev.* **119**, 7673–7717 (2019)
  8. A. Sivakumar, S.A. Martin Britto Dhas, Shock-wave-induced nucleation leading to crystallization in water. *J. Appl. Cryst* **52**, 1016–1021 (2019)
  9. A. Sivakumar, C. Victor, M. Muralidhr Nayak, S.A. Martin Britto Dhas, Structural, optical, and morphological stability of ZnO nano rods under shock wave loading conditions. *Mater. Res. Express* **6**, 045031 (2019)
  10. W. Paulus, I.A. Rahman, A. Jalar, N.K. Othman, R. Ismail, W.Y. Wan Yusoff, M. Abu Bakar, The Relationship between XRD Peak Intensity and Mechanical Properties of Irradiated Lead-Free Solder. *Mater. Sci. Forum* **888**, 423–427 (2016)
  11. M.A. Ahlam, M.N. Ravishankar, N. Vijayan, G. Govindaraj, V. Upadhyaya, A.P. Gnana Prakash, The effect of Co-60 gamma irradiation on optical properties of some nonlinear optical (NLO) single crystals. *J. Opt.* **41**, 158–166 (2012)
  12. N.C. Fernelius, F.K. Hopkins, M.C. Obmer, Nonlinear optical crystal development for laser wavelength shifting at AFRL Materials Directorate. *SPIE* **3793**, 1–7 (1999)
  13. J. Wang, H. Yu, Y. Wu, R. Boughton, Recent developments in functional crystals in china. *Engineering* **1**, 192–210 (2015)
  14. A. Saranraj, S. Sahaya Jude Dhas, M. Jose, P. Karuppasamy, M. Senthil Pandian, P. Ramasamy, S.A. Martin Britto Dhas, Investigation on the impact of xylenol orange dye on the growth and properties of unidirectional grown KDP crystals for photonic applications. *J. Cryst. Growth* **523**, 125154 (2019)
  15. A. Sivakumar, S. Suresh, S. Balachandar, J. Thirupathy J. Kalyana Sundar, S.A. Martin Britto Dhas; Effect of shock waves on thermophysical properties of ADP and KDP crystals. *Optics. Laser Tech* **111**, 284–289 (2019)
  16. A. Sivakumar, S. Sahaya Jude Dhas, S. Balachandar, S.A. Martin Britto Dhas, Effect of shock waves on structural and dielectric properties of ammonium dihydrogen phosphate crystal. *Z. Kristallogr.* (1–12) (2019)
  17. A. Sivakumar, A. Saranraj, S. Sahaya Jude Dhas, M. Jose, K. Kamala Bharathi, M. Britto Dhas, Modification of optical properties of ammonium dihydrogen phosphate crystal by employing shock waves. *Opt. Eng.* **58**, 107101 (2019)
  18. A. Sivakumar, S. Suresh, J. Anto Pradeep, S. Balachandar, S.A. Martin Britto Dhas, Effect of shock waves on dielectric properties of KDP crystal. *J. Electron. Mater.* **47**, 4381–4389 (2018)
  19. A. Sivakumar, A. Saranraj, S. Sahaya Jude Dhas, M. Jose, S.A. Martin Britto Dhas, Shock wave-induced defect engineering for investigation on optical properties of triglycine sulfate crystal. *Opt. Eng.* **58**, 077104 (2019)
  20. A. Sivakumar, S. Reena Devi, J. Thirupathy, R. Mohan Kumar, S.A. Martin Britto Dhas, Effect of shock waves on structural, thermophysical and dielectric properties of glycine phosphate (GPI) crystal. *J. Electron. Mater.* **48**, 7216–7225 (2019)
  21. A. Sivakumar, A. Saranraj, S. Sahaya Jude Dhas, S.A. Martin Britto Dhas, Shock wave induced enhancement of optical properties of benzil. *Cryst. Mater. Res. Express* **6**, 046205 (2019)
  22. A. Sivakumar, M. Sarumathi, S. Sahaya Jude Dhas, S.A. Martin Britto Dhas, Enhancement of the optical properties of copper sulfate crystal by the influence of shock waves. *J. Mater. Res.* (2020). <https://doi.org/10.1557/jmr.2019.383>
  23. A. Sivakumar, P. Eniya, S. Sahaya Jude Dhas, J. Kalyana Sundar, P. Sivaprakash, S. Arumugam, S.A. Martin Britto Dhas, Shock wave induced defect engineering on structural and optical properties of pure and dye doped potassium dihydrogen phosphate crystals. *Z. Kristallogr.* (2020). <https://doi.org/10.1515/zkri-2020-0017>
  24. A. Sivakumar, S. Sahaya Jude Dhas, S.A. Martin Britto Dhas, Shock wave-induced optical band gap engineering on pure and dye-doped potassium dihydrogen phosphate crystals. *J. Mater. Sci.: Mater. Electron.* (2020). <https://doi.org/10.1007/s10854-020-03928-0>
  25. C. Wickleder, P. Larsen, Crystal structure, second harmonic generation, and vibrational spectroscopy of K<sub>2</sub>Mg<sub>2</sub>(-SCN)<sub>6</sub>·3H<sub>2</sub>O. *Chem. Mater.* **16**, 4016–4021 (2004)



26. Y.Y. Wei, B. Tinant, J.-P. Declercq, M. Van Meerssche, J. Dale, Crown ether complexes of alkaline-earth metal ions. III. Structures of 1,4,7,10,13,16-hexaoxacyclooctadecane (18-crown-6) complexed with magnesium and barium thiocyanates. *Acta Cryst. C* **44**, 77–80 (1988)
27. S. Gunasekaran, S. Ponnusamy, Growth and characterization of cadmium magnesium tetra thiocyanate crystals. *Cryst. Res. Technol.* **41**, 130–137 (2006)
28. A. Sivakumar, S. Balachandar, S.A. Martin Britto Dhas, Measurement of “Shock Wave Parameters” in a novel table-top shock tube using microphones. *Hum. Fact. Mech. Eng. Defense. Saf.* **4**, 3 (2020)
29. E.V. Boldyreva, High-pressure studies of the hydrogen bond networks in molecular crystals. *J. Mol. Struct.* **700**, 151 (2004)
30. A.S. eed Hassanien, I.M. El Radaf, Optical characterizations of quaternary  $\text{Cu}_2\text{MnSnS}_4$  thin films: novel synthesis process of film samples by spray pyrolysis technique. *Physica B* **585**, 412110 (2020)
31. I.M. El Radaf, H.Y.S. Al-Zahrani, A.S. Hassanien, Novel synthesis, structural, linear and nonlinear optical properties of p-type kesterite nanosized  $\text{Cu}_2\text{MnGeS}_4$  thin films. *J. Mater. Sci.: Mater. Electron.* (2020). <https://doi.org/10.1007/s10854-020-03369-9>

**Publisher’s Note** Springer Nature remains neutral with regard to jurisdictional claims in published maps and institutional affiliations.